Inorganica Chimica Acta 363 (2010) 1455–1461

Contents lists available at ScienceDirect

Inorganica Chimica Acta

journal homepage: www.elsevier.com/locate/ica

Synthesis and redox properties of dinuclear rhodium(II) carboxylates with 2,6-di-*tert*-butylphenol moieties

Elena R. Milaeva [a,*], Natalia N. Meleshonkova [a], Dmitry B. Shpakovsky [a], Kirill V. Uspensky [a], Alexander V. Dolganov [a], Tatiana V. Magdesieva [a], Alexander V. Fionov [a], Alexey A. Sidorov [b], Grigory G. Aleksandrov [b], Igor L. Eremenko [b]

[a] Chemistry Department Moscow State Lomonosov University, Lenin Hill 1-3, Moscow, 119991, Russian Federation
[b] N.S. Kurnakov Institute of General and Inorganic Chemistry, Russian Academy of Sciences, Leninsky pr., 31, Moscow, 119991, Russian Federation

ARTICLE INFO

Article history:
Received 16 July 2009
Received in revised form 15 January 2010
Accepted 22 January 2010
Available online 29 January 2010

Keywords:
Dirhodium carboxylates
Rhodium(II)
2,6-Di-*tert*-butyl-4-cyanophenol
Phenoxyl radical
ESR
Cyclic voltammetry
Electron transfer

ABSTRACT

By exploiting the peculiar reactivity of $[Rh_2(\mu\text{-}O_2CBu^t)_4(H_2O)_2]$ (**1**) the examples of dinuclear rhodium(II) carboxylates containing N-donor axial ligands (**2**, **3**) $[Rh_2(\mu\text{-}O_2CBu^t)_4L_2]$ [where *L* = benzonitrile (**2**), 3,5-di-*tert*-butyl-4-hydroxybenzonitrile (**3**)] were synthesized and characterized by elemental analysis, IR, multinuclear NMR spectroscopy, MALDI-TOF mass spectrometry. It was found by X-ray diffraction that pairs of **3** in crystals are associated through H atoms of phenol groups to produce a dimer of dimers. The chemical oxidation of dirhodium complexes with 2,6-di-*tert*-butyl-4-cyanophenol pendants studied by means of ESR method in solutions leads to the formation of phenoxyl radicals **3′** in dirhodium system. The ESR data show the interaction of the unpaired electron with ligand nuclei (^1H, ^{14}N) and ^{103}Rh. The stability of radical complexes with phenoxyl fragments in axial position is influenced by the temperature. The enthalpy of the **3′** decomposition followed by the formation of cyanophenoxyl radical as 20 ± 1 kJ/mol was estimated. Redox transformations in dirhodium system including both metal and axial ligands were investigated by electrochemistry. CV experiments confirm the assumption of the metal oxidation ($Rh^{II} \rightarrow Rh^{III}$) as the first step following by the oxidation of the ligand.

1. Introduction

Dirhodium tetracarboxylates, $Rh_2(\mu\text{-}O_2CR)_4L_2$ with various axial ligands containing a variety of strong N, O, P bases L have long been known [1], and their paddlewheel structure, bonding, and reactivity have been extensively investigated [2–5]. Dirhodium complexes are of interest because of their applications in the field of material science and nanotechnology [6,7]. The use of dirhodium salts as catalysts for C–C bond formation in cycloaddition reactions of olefins [8], acetylenes [9] or in ring-forming C–H insertion reactions [10] has become such powerful synthetic tool as the development of highly enantioselective chiral Rh(II) catalysts [11].

Additionally, recent results achieved in the molecular design and focused synthesis of metal-based drugs suggest that transition metal complexes are promising anti-tumor agents [12]. Studies of the biological activity of dirhodium complexes support the assumption that dirhodium tetracarboxylates act as antibacterial agents, exhibit cytostatic activity against tumors [13] and a significant in vivo antitumor activity [14].

Although the precise anti-tumor mechanism of dirhodium carboxylate compounds has not been elucidated, it is known that they bind to DNA nucleobases and exhibit a strong preference for axial binding of guanine due to the hydrogen bonding interactions between the exocyclic amine group and a carboxylate oxygen atom [15–18]. A systematic variation of the axial and equatorial ligands has shed light on the structure-activity relationship in this family of compounds. It has been shown, for instance, that the anti-tumor activity increases in the series $Rh_2(\mu\text{-}O_2CR)_4$ (R = Me, Et, Pr) with the increase of lipophilicity of the R group [19]. Moreover, since there is the increasing evidence that the oxidative stress plays a critical role in certain pathological states including cancer the application of antioxidants in cancer therapy is strongly needed [20].

The metal complexes containing antioxidative groups of 2,6-di-*tert*-butylphenols have shown the activity as antioxidants, inflammatory agents, scavengers for reactive oxygen species [21–25] which makes them promising agents in complex cancer therapy.

We believe that a systematic research is needed in order to get more insight into complexation of lipophilic phenolic pendants by dirhodium(II) carboxylate molecules, as these interactions play an important role in design of new polytopic redox systems.

* Corresponding author. Tel.: +7 495 9393864; fax: +7 495 9395546.
E-mail address: milaeva@org.chem.msu.ru (E.R. Milaeva).

0020-1693/$ - see front matter © 2010 Published by Elsevier B.V.
doi:10.1016/j.ica.2010.01.029

Previously we demonstrated that the introduction of 2,6-di-*tert*-butulphenols into the ligand environment of transition metal increases the stability of corresponding phenoxyl radicals due to the interaction of the unpaired electron with the metal center [26].

In the present paper we report on the synthesis, characterization and redox properties of dirhodium complexes with 2,6-di-*tert*-butulphenol moiety in the ligand $[Rh_2(\mu\text{-}O_2CBu^t)_4L_2]$, where L = 3,5-di-*tert*-butyl-4-hydroxybenzonitrile (**3**) and its analogue $[Rh_2(\mu\text{-}O_2CBu^t)_4L_2]$, where L = benzonitrile (**2**).

The X-ray crystal structure of phenol containing complex (**3**) is described as well. We found by ESR that the chemical oxidation of **3** leads to phenoxyl radicals, the stability of which depends on temperature. We also studied electrochemical properties of dirhodium complexes.

2. Experimental

2.1. Materials and equipment

The starting complex $[Rh_2(\mu\text{-}O_2CCBu^t)_4(H_2O)_2]$ (**1**) [27] and 3,5-di-*tert*-butyl-4-hydroxybenzonitrile [28] were prepared according to literature procedures. All other chemicals are commercially available and used as supplied. $CDCl_3$ (Merck) was used without further purification; other solvents were routinely distilled and dried prior to use. Elemental analysis was performed in the Laboratory of Microanalysis at the Moscow State Lomonosov University (Moscow), Russia.

Infrared spectra were recorded on KBr pellets or in CH_2Cl_2 solution with a "IR200 (Thermo Nicolet)" spectrometer. Electronic absorption spectra were measured on a Cari 219 Varian spectrophotometer.

The ^1H, ^{13}C NMR measurements were performed with a Bruker Avance-400 spectrometer operating on 400 or 100 MHz, respectively in $CDCl_3$.

The MALDI-TOF spectra were acquired using a Autoflex II (Bruker daltonics) mass spectrometer. The samples were dissolved in $CHCl_3$ with 2,5-dihydroxybenzoic acid (DHB) as matrix and put at target.

ESR spectra were recorded on the Bruker EMX spectrometer at X-band frequency (9.8 GHz). The measurements were carried out after pre-evacuation 10^{-2} Torr) of tubes with solutions of samples (concentration $1\cdot10^{-4}$ Mol L^{-1}). The oxidant PbO_2 (Aldrich) was taken in a tenfold excess.

Cyclic voltammetry experiments were performed in CH_3CN solution with 0.05 M Bu_4NBF_4 as supporting electrolyte using a model IPC-Win potentiostat in a conventional one - compartment three-electrode cell (10 ml of solution). A platinum working electrode, platinum wire auxiliary electrode and aqueous Ag/AgCl/KCl reference electrode were used. The electrode was thoroughly polished and rinsed before measurements. The measurements were performed at scan rate equal to 100 mV s^{-1}. The formal potential of the ferrocene Fc/Fc^+ couple versus RE in the dichloromethane solution is equal to 550 mV. All solutions were thoroughly deaerated before and during the CV experiments using argon gas.

2.2. Syntheses

2.2.1. $[Rh_2(\text{-}O_2CBu^t)_4(PhCN)_2]$ (**2**)

To a suspension of **1** (0.200 g, 0.310 mmol) in 10 ml toluene benzonitrile (0.070 g, 0.679 mmol) was added. The solid phase immediately dissolved after addition of benzonitrile. The color of solution immediately changed from pale green to purple. The solution was left for 1 h. The solvent was slowly removed in vacuum, the resulting brown-red crystals were washed with hexane and dried in the air. Yield 0.197 g (85%). *Anal.* Calc. for $C_{34}H_{46}N_2O_8Rh_2$: C, 50.01; H, 5.68; N, 3.43. Found: C, 50.07; H, 5.39; N, 3.64%.

IR (KBr pellet, cm^{-1}): 1583 (vs), 1483 (m), 1414 (s), 1223 (s), ν(CN) 2249 (w), ν(CH) 2871–2962 (s). MS (MALDI-TOF), *m/z*: 610 $[C_{20}H_{36}O_8Rh_2]^+$.

^1H NMR ($CDCl_3$): 1.03 (s, 36 H, $C(CH_3)_3$); 7.56 (t, 4H, Ph), 7.70 (t, 2H, Ph), 7.85 (d, 4H, Ph).

^{13}C NMR: 27.74 ($OOCC(CH_3)_3$); 40.55 ($OOCC(CH_3)_3$); 112.46; 117.27; 129.18; 132.67; 133.13 (C-arom); 117.27 (CN), 198.48 (C=O).

UV–Vis spectrum (EtOH), lg ε (λ_{max}/nm): 4.32 (249); 2.63 (422); 2.62 (590).

2.2.2. $[Rh_2(\text{-}O_2CBu^t)_4L_2]$ (**3**)

To a solution of **1** (0.265 g, 0.410 mmol) in 3 ml toluene 3,5-di-*tert*-butyl-4-hydroxybenzonitrile (0.200 g, 0.865 mmol) was added. The color of solution immediately changed from pale green to dark blue. The solution was stirred for 15 min. The solvent was partially removed by evaporation, and then 2 ml of benzene were added and left for crystallization on the air. Purple crystals of **2** were collected after precipitation by filtration, washed with hexane and dried in the air. Yield 0.303 g (69%). *Anal.* Calc. for $C_{50}H_{78}N_2O_{10}Rh_2$: C, 55.97; H, 7.33; N, 2.61. Found: C, 56.27; H, 6.97; N, 2.40%.

IR (KBr pellet, cm^{-1}): 1585 (vs), 1482 (m), 1414 (s), 1223 (s), ν(CN) 2246 (w), ν(CH) 2873–2960 (s), ν(OH associated) 3546 (w), ν(OH non-associated) 3623 (w).

^1H NMR ($CDCl_3$): δ (ppm): 1.03 (s, 18 H, $C(CH_3)_3$); 1.48 (s, 18 H, $C(CH_3)_3$); 5.62 (s, 1 H, OH); 7.36 (s, 2H, C_6H_2).

^{13}C NMR: 27.69 ($OOCC(CH_3)_3$); 29.89 ($ArC(CH_3)_3$); 34.43 ($OOCC(CH_3)_3$); 40.41 ($ArC(CH_3)_3$); 103.01, 129.96, 136.98, 158.00 (C-arom.); 118.01 (CN), 198.48 (C=O).

Table 1
Crystallographic data and structure refinement for $[Rh_2(\mu\text{-}O_2CBu^t)_4L_2]\cdot4C_6H_6$. (**3**·$4C_6H_6$, L= 3,5-di-*tert*-butyl-4-hydroxybenzonitrile).

Formula	$C_{74}H_{102}N_2O_{10}Rh_2$
Formula weight	1385.40
T (K)	120(2)
λ (Å)	0.71073
Crystal system	triclinic
Space group	$P\bar{1}$
Unit cell dimensions	
a (Å)	12.755(6)
b (Å)	12.939(9)
c (Å)	13.725(6)
α (°)	66.93(4)
β (°)	67.18(3)
γ (°)	81.67(4)
V (Å^3)	1920.7(18)
D_{calc} (Mg/m3)	1.198
Absorption coefficient (mm^{-1})	0.482
F(0 0 0)	730
Crystal size (mm)	0.35 × 0.23 × 0.15
Theta range for data collection (°)	1.71–28.25
Limiting indices	$-8 \leqslant h \leqslant 12$, $-12 \leqslant k \leqslant 17$, $-18 \leqslant l \leqslant 16$
Reflections collected/unique	13 655/9421 [R_{int} = 0.0625]
Completeness to theta	28.25 93.5%
Maximum and minimum transmission	0.9312 and 0.8494
Refinement method	Full-matrix least-squares on F^2
Data/restraints/parameters	9421/0/424
Goodness-of-fit (GOF) on F^2	1.014
Final R indices [$I > 2\sigma(I)$]	R_1 = 0.0671, wR_2 = 0.1794
R indices (all data)	R_1 = 0.0724, wR_2 = 0.1827
Largest difference in peak and hole (e A^{-3})	1.352 and −1.640

UV–Vis spectrum (EtOH), lg ε (λ_{max}/nm): 3.7 (250); 2.3 (449); 2.5 (594).

Mass spectrum (MALDI-TOF), *m/z*: 610 $[C_{20}H_{36}O_8Rh_2]^+$.

The crystals of **3** were suitable for a single-crystal X-ray structure determination.

2.3. Crystallographic data collection and structure determination

Crystallogrphic data for **3** were collected by usual procedure [29] using a Bruker AXS SMART 1000 diffractometer equipped with CCD detector (graphite-monochromated Mo Kα radiation, λ = 0.7107 Å, T = 120 K, ω scan mode, scan step – 0.3°, time of frames collection – 30 s, $2\theta_{max} \leqslant 60°$). The semiempirical absorption correction was applied [30]. The structure was solved by direct methods using the SHELXS97 [31] program and refined using the SHELXL97 package [32] by least-squares method in the full-matrix anisotropic (atoms C(8), C(9) and C(10) are disordered and every atom occupied two equivalent position with populated ~0.5) approximation. The crystallographic data for **3** are summarized in Table 1.

3. Results and discussion

3.1. Synthesis

According to the typical axial reactivity of $[Rh_2[\mu\text{-}O_2CBu^t)_4(H_2O)_2]$ (**1**) novel dirhodium complexes $[Rh_2(\mu\text{-}O_2CBu^t)_4L_2]$, where L = benzonitrile (**2**) and its analogue $[Rh_2(\mu\text{-}O_2CBu^t)_4L_2]$, where L = 3,5-di-*tert*-butyl-4-hydroxybenzonitrile (**3**) were synthesized. Complexes **2** and **3** were obtained in high yield by treatment of **1** with two equivalents of benzonitrile or 3,5-di-*tert*-butyl-4-hydroxybenzonitrile, respectively (Scheme 1).

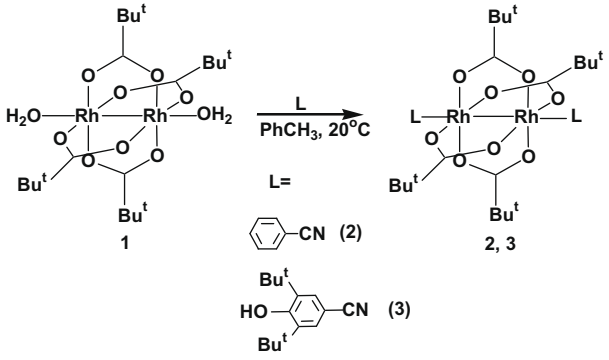

Scheme 1.

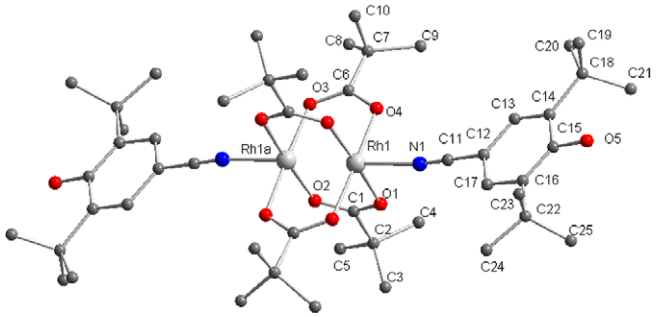

Fig. 2. Molecular structure of Complex **3**.

Compounds **2**, **3** were isolated as purple solids stable in the air and in solutions. They were characterized by means of elemental analyses, MALDI-TOF mass spectra, IR and ^1H, ^{13}C NMR spectroscopy, the complex **3** was analyzed by X-ray diffraction.

The solid IR spectra of complexes **1**–**3** exhibit similar ν_{asym}(COO) bands at 1583–1585 cm^{-1}. The shifts of characteristic ν(CN) absorption bands for **2**, **3** at 2249–2246 cm^{-1} to a region of higher frequencies ($\Delta\ \nu$(CN) ≈ 21 cm^{-1}) when compared with non-coordinated ligands confirm the N-coordination of axial ligands in dirhodium complexes.

In the IR spectrum of **3** in KBr there are two absorptions in the region of 3623–3546 cm^{-1} (Fig. 1). The first characteristic narrow band at 3623 cm^{-1} is assigned to the free hindered phenol group and another wide one at 3546 cm^{-1} is related to hydrogen bonds formation between phenol group and neighboring carboxylate moiety of the complex molecule that is nontrivial for hindered phenols. On the contrary, the only one free O–H group absorption at 3620 cm^{-1} was observed in IR spectrum of CH_2Cl_2 solution of **3**.

As it is well known in non-coordinating and non-polar solvents the phenol group in sterically hindered phenols is not involved in hydrogen bond formation and the bands corresponding to non-associated OH group in the IR spectra are registered in the region

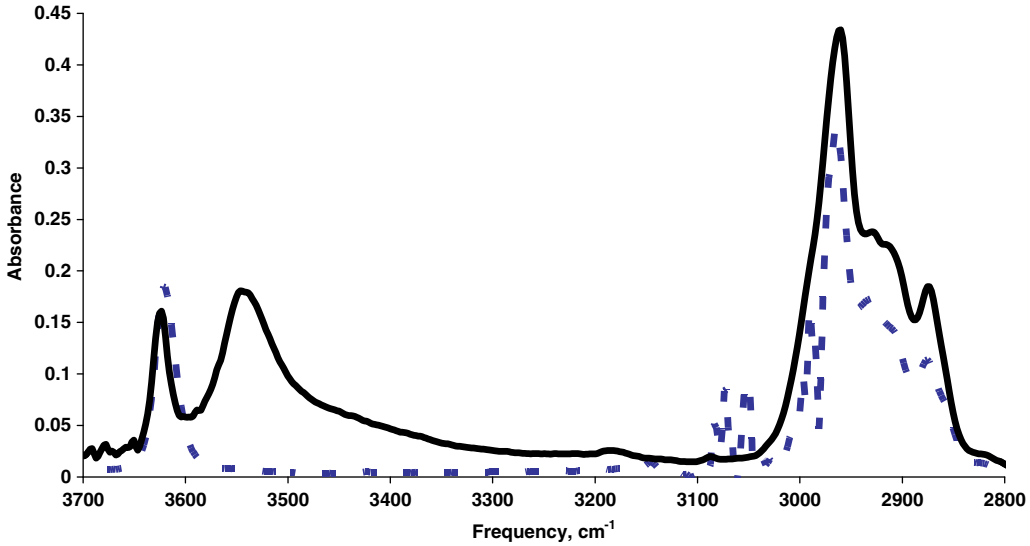

Fig. 1. IR spectrum of **3** in KBr pellets (solid line) and in CH_2Cl_2 solution (dashed line).

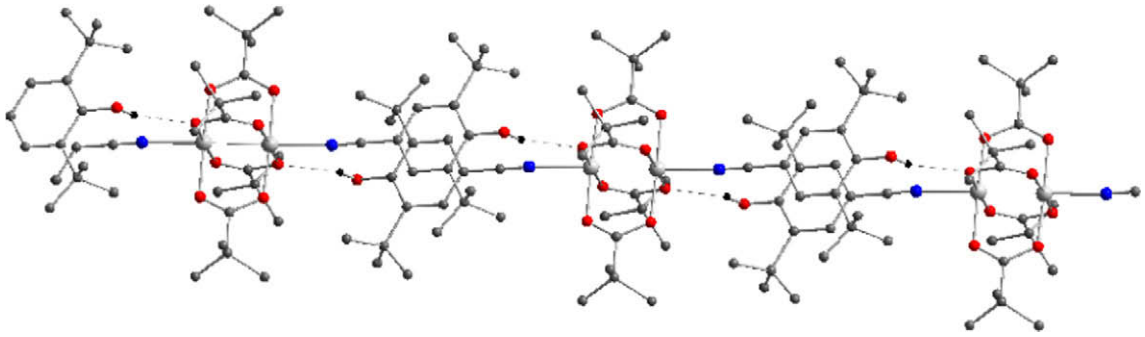

Fig. 3. Crystal packing of Complex **3**.

of 3600–3650 cm^{-1} [33]. Therefore, **3** does not associate in non-polar solvents.

On the contrary, the only one free O–H group absorption at 3620 cm^{-1} was observed in IR spectrum of CH_2Cl_2 solution of **3**. Therefore, **3** does not associate in non-polar solvents.

These data was supported by X-ray diffraction investigation of complex **3** (Figs. 2 and 3).

The structure of binuclear complex $[Rh_2(\mu\text{-}O_2CBu^t)_4L_2]$ (**3**) was determined for solvate with 4 molecules of the benzene. All four solvate molecules have crystallographic symmetry C_i, Complex **3** have crystallographic symmetry C_i also. In the crystal molecules of **3** are assembled in infinite ribbons along axis z: each hydrogen atom of phenol group is bonded to oxygen atom O(1) of neighboring carboxylate group (O5–H5 0.84 Å, H···O 2.20 Å, O–H···O 140°, O(5)···O1 [−x, −y, −z + 1] 2.901 (5) Å) .

Selected bond length and bond angles of **3** are summarized in Table 2. The unit N–Rh–Rh–N has appeared slightly distorted from linear geometry. The values of Rh–Rh and Rh–O bonds distances for **3** correspond to that of **1**. The length of Rh–Rh and Rh–O in dirhodium complex **1** with H_2O as axial ligands are 2.371 (1) Å and 2.036 (2), respectively [4,27]. The complex $Rh_2(OOCMe_3)_4(H_20)_2$ crystallizes in the triclinic space group $P\bar{1}$ with one formula weight in the unit cell. Four pivalate groups bridge the dirhodium(II) unit which is located about a crystallographic center of inversion. Two oxygen atoms of water molecules coordinate to the Rh atoms via the axial positions with Rh–O distances of 2.295 (2) Å. There are several examples of dirhodium complexes with distorted from linear geometry of L–Rh–Rh–L unit such as dirhodium pivalates with hindered axial ligands [1] and complexes with non-equal equatorial ligands, e.g., $Rh_2(Bu^tCO_2)_3(TTFCO_2)L_2$ and $Rh_2(Bu^tCO_2)_2(TTFCO_2)L_2$, where $TTFCO_2$ = tetrathiafulvalene carboxylate [34].

The data of electronic absorption spectroscopy show the presence of π–π^* transition in the aromatic systems of **2** and **3** in the region of 220–230 nm and transitions π^*→Rh–O σ^* (420–450 nm)

Table 2
Selected bond length (Å) and angles (°) for **3.**

Bond lengths	Bond angles
Rh–Rh′ 2.3897(14)	RhRhN 177.11(12)
Rh–N 2.237(5)	RhNC 168.0(5)
Rh–O 2.008(4)	ORhN 89.34(16)
2.019(4)	91.89(17)
2.038(4)	91.34(17)
2.041(4)	95.03(16)

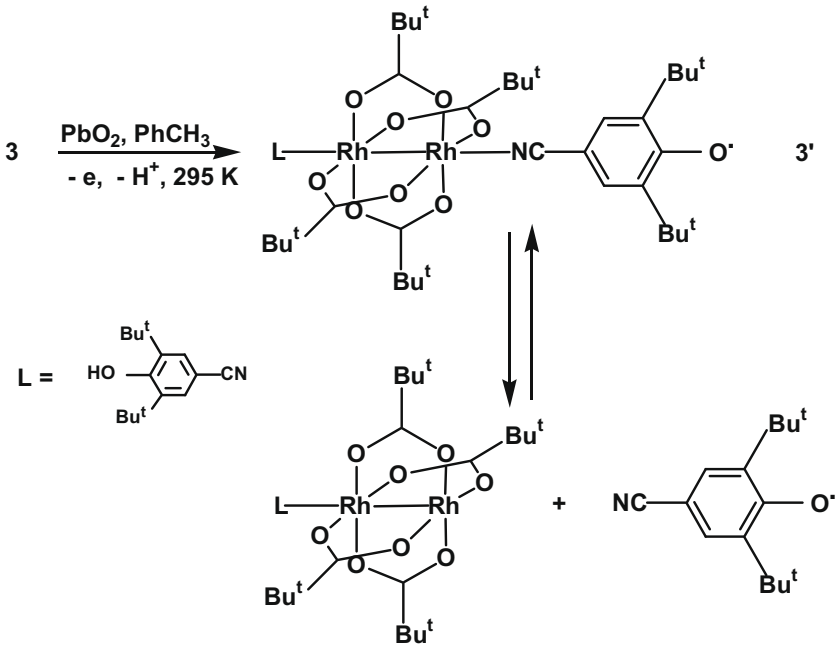

Scheme 2.

and in region of 590–595 nm assigned to $\pi^*(Rh_2) \rightarrow \sigma^*(Rh_2)$ as it was denoted in the case of similar complex $[Rh_2(O_2CMe)_4(H_2O)_2]$. The location of the Rh–Rh δ^* orbital just above the π^* implies that there should be a dipole-forbidden vibronically allowed transition just below the Rh–Rh $\pi^* \rightarrow$ Rh–Rh σ^* transition at 578 nm assigned to $\delta^* \rightarrow \sigma^*$ [4,35].

As it follows from the spectral data, no oxidation of phenol substituents to the quinoid derivatives occurs in the synthesis of **3**.

The chemical oxidation of phenol fragment in complex **3** was carried out by lead dioxide in toluene to generate phenoxyl radical **3′** (Scheme 2).

The X-band ESR measurements (at 295 K) have shown the superposition of two spectra for oxidation product of **3** (Fig. 4a). The first spectrum (g = 2.0043, a(N) = 1.345 G, a(2H)= 2.18 G) corresponds to free 2,6-di-*tert*-butyl-4-cyanophenoxyl radical described in the literature [28]. On the other hand, it was reported that the oxidation of Rh(III) complex with N-coordinated 4-hydroxy-3,5-di-*tert*-butylbenzonitrile leads to the formation of the corresponding phenoxyl-centered radical [36]. No interaction of the unpaired electron with the metal nucleus was observed and the hyperfine coupling (hfc) constants [a(2H), a(N)] are typical for the organic phenoxyl radical.

In the case of radical 3′ we have observed the interaction of the unpaired electron with only one Rh nuclei and the number of lines, intensity, hyperfine coupling constant do not correspond to the signal observed for Rh_2^{5+}-centered species [34].

It was also reported that the hyperfine splitting constant from the second rhodium nuclei may be several time smaller than that of first one, so it could not be detected in spectrum of radical. The ESR spectrum of the Lewis acid-base adduct of the rhodium trifluoroacetate dimer and 2,2,6,6-tetramethylpiperidine-N-oxyl was reported. The spectrum of the complexed nitroxide demonstated a remarkable g-value shift, compared to the uncomplexed base, and as well as a rhodium hyperfine coupling of 1.7 G with only one rhodium [4,37].

The second spectrum (g = 2.0084, a(N) = 2.06 G, a(2H) = 2.06 G, a(^{103}Rh) = 0.8 G) was assigned to a spectrum of paramagnetic complex **3′**. The experimental and simulated ESR spectra are in good correlation to each other (Fig. 4). So, ESR spectrum of **3′** showed that the spin density is distributed between the organic moiety (including nitrogen atom of nitrile group and two meta-protons of the phenoxyl ring) and the metal (one rhodium atom). The radical **3′** is stable at room temperature in the absence of oxygen for several days.

It is worth to note that despite the presence of two phenol groups the only monoradical species were detected after the oxidation of **3** as it has been shown previously for dimers of π-allyl complexes [38] and tetraphenol substituted metallophthalocyanines [39]. Therefore no spin-spin interaction was detected in this case as well.

According to the ESR data the stability of radical **3′** confirms the possible cleavage of metal-ligand bond and formation of free cyanophenoxyl radical in solution, that has been observed previously for mononuclear rhodium nitrile complexes [36].

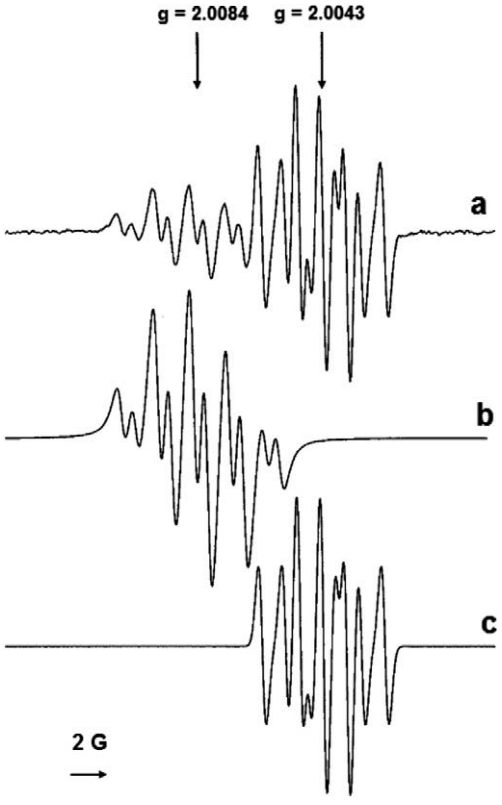

Fig. 4. ESR spectra (T = 295 K) observed after oxidation of **3** by PbO_2 in toluene (a – experimental; b – simulated with parameters g = 2.0084, a(N)= 2.06 G, a(2H)= 2.06 G, a(^{103}Rh)= 0.8 G; c – simulated with parameters g = 2.0043, a(N) = 1.345 G, a(2H) = 2.18 G).

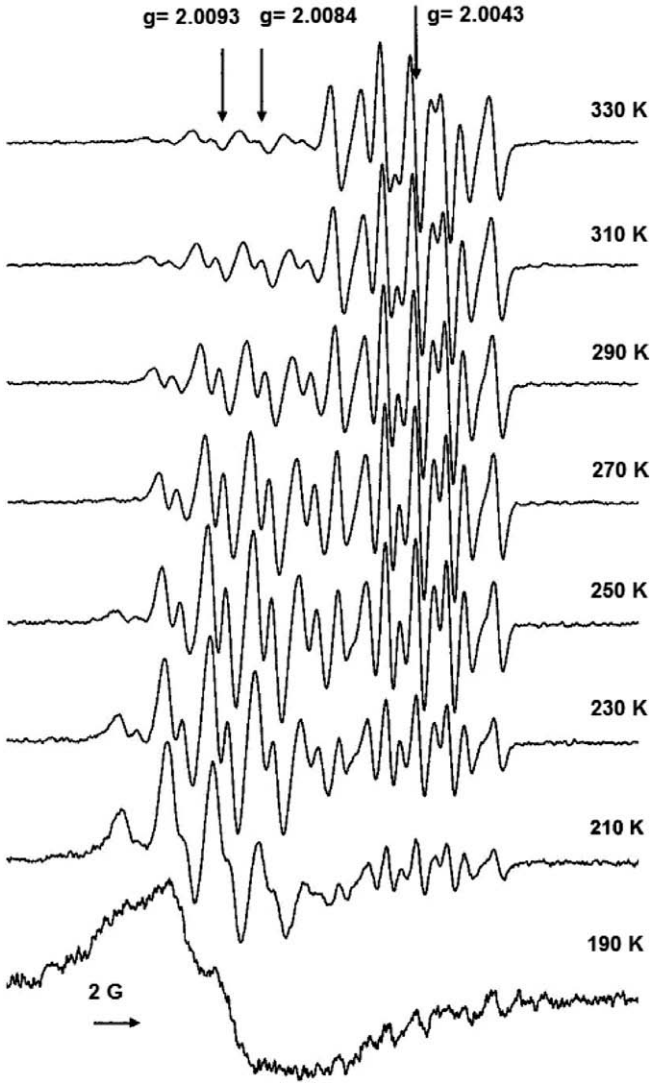

Fig. 5. Temperature dependence of the ESR spectrum of oxidation product of **3** (PbO_2, toluene, 190–330 K).

Table 3
Oxidation and reduction peak potential values for **1–3**. (Pt, C = 0.7 mM, 0.05 M Bu_4NBF_4, vs. Ag/AgCl/KCl, 0.1 V s^{-1}).

Compound	$E1_{ox}$ (V)	$E2_{ox}$ (V)	E_{red} (V)
1	1.20/1.15		−1.14
2	1.20/1.15		−1.21
3	1.23/1.15	2.04 2.07	−1.08

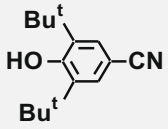

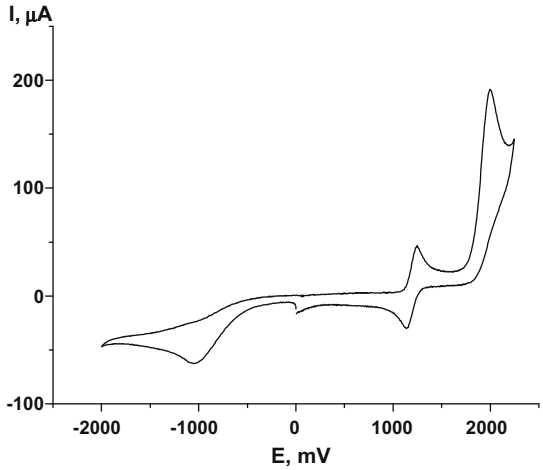

Fig. 6. Cyclic voltammogram of **3** in Ar saturated solution (Pt, CH_3CN, C = 0.7 mM, 0.05 M Bu_4NBF_4, vs. Ag/AgCl/KCl, scan rate 0.1 Vs^{-1}).

The intensities of both signals in ESR spectrum depend on temperature. The intensity of signal of **3′** decreases with the increase of free cyanophenoxyl radical signal during the heating of the solution. The decomposition of radical **3′** is accompanied by the elimination of 2,6-di-*tert*-butyl-4-cyanophenoxyl radical and, probably, the compensation of rhodium vacant axial position by coordination of donor atoms of neighboring carboxylate groups (Scheme 2).

The temperature dependence of ESR spectra has been studied in the range of temperatures from 330 K to 190 K (Fig. 5). The dependence of two radicals integral intensities ratio on T^{-1} has demonstrated a linear function (in the temperature range 260–330 K). This allowed to estimate the enthalpy of the **3′** decomposition followed by the formation of cyanophenoxyl radical as 20 ± 1 kJ/mol.

Thus, the oxidation of dirhodium complex **3** with redox fragments leads to the temperature-controlled equilibrium between dirhodium moiety and N-donor paramagnetic ligand. It is worth to note that g-factor of radical 3′ is also temperature dependent and increases with the temperature decrease. At 190 K the wide signal was observed with g = 2.0093. It could be proposed that at low temperature this signal corresponds to biradical species.

Important information about the properties of complexes **1–3** can be obtained from their electrochemical investigation. Electrochemical oxidation and reduction potential values for phenol-containing complex **3** as well as for model complexes **1** and **2** measured using cyclic voltammetry are presented in Table 3.

The first oxidation peak for complexes **1–3** is one-electron one and reversible, as follows from the ratios of peak currents for direct (anodic) and reverse (cathodic) peaks *Ia*/*Ic* which are equal to 1 at the applied potential scan rates. The peak separation values (ΔE_p) fall within the interval of 50–80 mV (in CH_3CN). The linear dependence $I_p - v^{1/2}$ (v = scan rate) indicates that the process is diffusionally controlled. The peak can be assigned to the formation of mixed-valence Rh^{2+}–Rh^{3+} complex with high delocalization of a charge over dirhodium fragment [40], without destruction of the dimeric cage structure, as it is confirmed by the CV data. In the case of **3**, an additional two-electron peak at the potential of 2.04 V (CH_3CN) can be observed (Fig. 6a), which more likely corresponds to the oxidation of 2,6-di-*tert*-butylphenol fragment. The irreversibility of the peak observed means that the electron transfer is followed by chemical reaction (Scheme 3). More likely it is a proton elimination from the initially formed phenoxyl radical-cation yielding phenoxyl radical which is easily further oxidized at a potential applied. The phenoxonium cation formed during the oxidation is unstable and can be easily involved in different chemical processes [41].

The reductive electrochemical behaviour of **1–3** is in a good agreement with that observed for analogous $Rh_2(NHCOCF_3)_4$ in which the LUMO is localized at the orbitals of Rh centers [42]. The reduction of complexes **1–3** is one-electron process and irreversible. The electrochemical experiments were carried out in coordinating polar CH_3CN. As follows from Table 3, both oxidation and reduction potential values do not differ significantly for **1–3** in CH_3CN, allowing to assume that the substitution of axial ligands by the molecules of solvent takes place in this case. The potential value for the second oxidation peak for **3** is very close to that observed for the free 3,5-di-*tert*-butyl-4-hydroxybenzonitrile taken for comparison. This is one more indication of the substitution of axial ligands in complexes **1–3** with the molecules of the solvent which proceeds in CH_3CN. Possibly, the redox properties

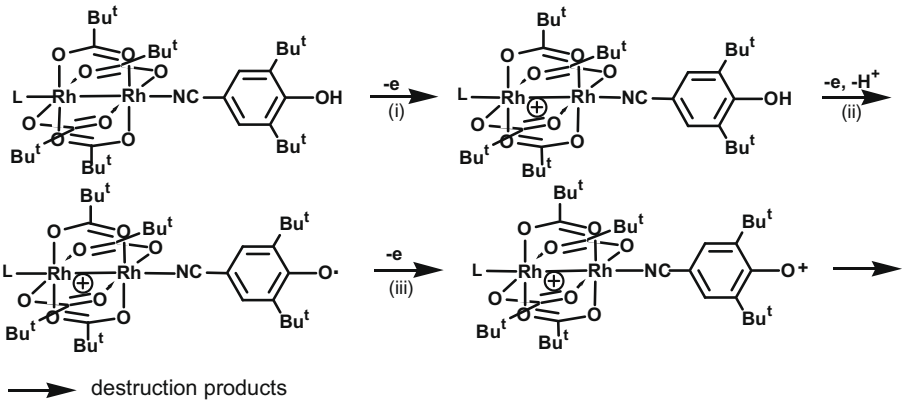

Scheme 3.

of dirhodium complexes are not essentially influenced by the nature of axial ligands due to the substantial involvement of the orbitals of Rh centers in the electrochemical oxidation and reduction processes. The same tendency was observed for the analogous Rh tetraacetate complexes with various axial ligands [43].

4. Conclusion

The novel coordination compound of dirhodium, containing 2,6-di-*tert*-butylphenol fragment in nitrile ligands was synthesized. The oxidation of this compound that leads to the phenoxyl radical formation in the ligand environment was studied. The relatively stable paramagnetic species formed in the redox transformations are ligand-centered radicals. The influence of the unpaired electron upon the coordination center, metal and metal–ligand bond has been observed. The intramolecular transformations in paramagnetic species formed in the oxidation of binuclear rhodium carboxylates were investigated by ESR.

It was found by electrochemical method (CVA) that the dirhodium carboxylates are politopic redox systems with two redox centers – both metal and ligand.

This result opens up the possibility for the design of novel biomimetic systems that might serve as electron and proton transfer agents in biological systems.

Acknowledgements

We gratefully acknowledge financial support from Russian Foundation for Basic Research (Grant No. 08-03-00844).

Appendix A. Supplementary material

CCDC 660536 contains the supplementary crystallographic data for **3**. These data can be obtained free of charge from The Cambridge Crystallographic Data Centre via http://www.ccdc.cam.ac.uk/data_request/cif. Supplementary data associated with this article can be found, in the online version, at doi:10.1016/j.ica.2010.01.029.

References

[1] A.A. Sidorov, G.G. Aleksandrov, E.V. Pakhmutova, A.Yu. Chernyad'ev, I.L. Eremenko, I.I. Moiseev, Russ. Chem. Bull. 54 (2005) 588.
[2] J. Hansen, H.M.L. Davies, Coord. Chem. Rev. 252 (2008) 545.
[3] H.T. Chifotides, K.R. Dunbar (Eds.), Rhodium Compounds, third ed.F.A. Cotton, C. Murillo, R.A. Walton (Eds.), Multiple, Bonds between Metal Atoms, Springer-Science and Business Media Inc., New York, 2005, p. 465. Chapter 12.
[4] E.B. Boyar, S.D. Robinson, Coord. Chem. Rev. 50 (1983) 109.
[5] T.R. Felthouse, Prog. Inorg. Chem. 29 (1982) 73.
[6] J.M. Lehn, Supramolecular Chemistry, VCH, New York, 1995.
[7] P.L. Boulas, M. Go'mez-Kaifer, L. Echegoyen, Angew. Chem., Int. Ed. 37 (1998) 216.
[8] P. Manitto, D. Monti, S. Zanzola, G. Speranza, Chem. Commun. (1999) 543.
[9] M.P. Doyle, M. Protopopova, P. Mueller, D. Ene, E.A. Shapiro, J. Am. Chem. Soc. 116 (1994) 8492.
[10] A. Srikrishna, S.J. Gharpure, Chem. Commun. (1998) 1589.
[11] M.P. Doyle, M.A. Mckervey, T. Ye, Modern Catalytic Methods for Organic Synthesis with Diazo Compounds, John Wiley, New York, 1998.
[12] M.J. Cleare, P.C. Hydes, in: H. Sigel (Ed.), Metal Ions in Biological Systems, vol. 11, Marcel Dekker, New York, 1980.
[13] F. Pruchnik, D. Dus, J. Inorg. Biochem. 61 (1996) 55.
[14] R.A. Howard, A.P. Kimball, J.L. Bear, Cancer Res. 39 (1979) 2568.
[15] H.T. Chifotides, K.M. Koshlap, L.M. Prez, K.R. Dunbar, J. Am. Chem. Soc. 125 (2003) 10703.
[16] D.V. Deubel, H.T. Chifotides, Chem. Commun. (2007) 3438.
[17] K.V. Catalan, J.S. Hess, M.M. Maloney, D.J. Mindiola, D.L. Ward, K.R. Dunbar, Inorg. Chem. 38 (1999) 3904.
[18] H.T. Chifotides, K.R. Dunbar, Acc. Chem. Res. 38 (2005) 146.
[19] R. Rahimi, S. Nikfar, B. Larijani, M. Abdollahi, Biomed. Pharmacother. 59 (2005) 365.
[20] E. Denisov, Handbook of Antioxidants, CRC Press, Boca Raton, New York, 1995.
[21] U.S. Patent, US 6127356 A3 03.10.00. SOD–, catalase– and peroxidase–mimetic porphyrin derivative oxidant scavengers, their preparation, and their therapeutic use. J.D. Crapo, I. Fridovich, T. Ouru, B.J. Day, J. Brian, R.J. Folz, B.A. Freeman, M.P. Trova, I. Batinik–Haberle (Duke University, USA). Appl. US 1996–663028, 07.06.96, p. 97.
[22] E.R. Milaeva, D. Shpakovsky, Yu. Gracheva, O. Gerasimova, V. Tyurin, V. Petrosyan, J. Porphyrins Phthalocyanines 8 (2003) 701.
[23] E.R. Milaeva, V.Yu. Tyurin, D.B. Shpakovsky, O.A. Gerasimova, Z. Jingwei, Yu.A. Gracheva, Heteroat. Chem. 17 (2006) 475.
[24] E.R. Milaeva, V.Yu. Tyurin, Yu.A. Gracheva, M.A. Dodochova, L.M. Pustovalova, V.N. Chernyshev, Bioinorg. Chem. Appl. (2006) 64927.
[25] E.R. Milaeva, J. Inorg. Biochem. 100 (2006) 905.
[26] E.R. Milaeva, Russ. Chem. Bull. 50 (2001) 573.
[27] F.A. Cotton, T.R. Felthouse, Inorg. Chem. 19 (1980) 323.
[28] E. Mueller, A. Riecker, R. Mayer, K. Scheffler, Ann 645 (1961) 36.
[29] SMART (control) and SAINT (Integration) software, version 5.0, Bruker AXS Inc., Madison, WI, 1997.
[30] G.M. Sheldrick, SADABS, program for scaling and correction of area detector data, University of Göttingen, Germany, 1997 (based on the method of R.H. Blessing, Acta Crystallogr., Sect. A 51 (1995) 33.).
[31] G.M. Sheldrick, SHELX97, Program for the Solution of Crystal Structures, Göttingen University, Göttinngen, Germany, 1997.
[32] G.M. Sheldrick, SHELXL97, program for the Refinement of Crystal Structures, University of Göttingen, Germany, 1997.
[33] K. Ingold, D. Taylar, Can. J. Chem. 39 (1961) 481.
[34] Masahiro Ebihara, Mitsuko Nomura, Shogo Sakai, Takashi Kawamura, Inorg. Chim. Acta. 360 (2007) 2345.
[35] J.G. Norman Jr., G.E. Renzoni, D.A. Case, J. Am. Chem. Soc. 101 (1979) 5256.
[36] A.Z. Rubezhov, E.R. Milaeva, A.I. Prokof'ev, I.V. Karsanov, O.Yu. Okhlobystin, Bull. Acad. Sci. USSR. Div. Chem. Sci. 33 (1984) 1050.
[37] R.M. Richman, T.C. Kuechler, S.P. Tanner, R.S. Drago, J. Am. Chem. Soc. 99 (1977) 1055.
[38] E.R. Milaeva, A.Z. Rubezhov, A.I. Prokof'ev, O.Yu. Okhlobystin, J. Organomet. Chem. 193 (1980) 135.
[39] E.R. Milaeva, G. Speier, Inorg. Chim. Acta 192 (1992) 117.
[40] D. Astruc, Electron Transfer and Radical Processes in Transition-Metal Chemistry, New York, VCH, 1995.
[41] B. Speiser, A. Rieker, J. Electroanal. Chem. 102 (1979) 373.
[42] K.M. Kadish, D. Lancon, A.M. Dennis, J.L. Bear, Inorg. Chem. 21 (1982) 2987.
[43] M.Y. Chavan, T.P. Zhu, X.Q. Lin, M.Q. Ahsan, J.L. Bear, K.M. Kadish, Inorg. Chem. 23 (1984) 4538.